Cubesat Power System Design for High Precision, Solar Observation

A project present to
The Faculty of the Department of Aerospace Engineering
San Jose State University

in partial fulfillment of the requirements for the degree
Master of Science in Aerospace Engineering

By

Daniel T. Hernandez

May 2015

approved by

Dr Marcus Murbach
Faculty Advisor

Cubesat Power System Design for High Precision, Solar Observation

Daniel T. Hernandez[1]
San Jose State University, San Jose, CA, 95112

There is much need for improvement upon the current mechanisms of space weather study and monitoring of solar activity. The purpose of this project is to design and build a low cost 3U cubesat, which will have 3-axis stability and continuously point at the sun. Brief introductions are made on general cubesat systems. State of the art cubesat technology is discussed including materials, solar cells, gyroscopes and sun sensors. A literature review entails descriptions of relevant cubesat missions. Orbital mechanics theory is discussed in order to predict the environment of the cubesat. Using specifications from the International Space Station, orbital parameters for the cubesat are calculated. Maximum power point tracking with battery bus topology is chosen for power regulation in order to account for temperature effects on solar cells due to LEO environment. TASC solar cells are chosen for power generation based on efficiency and flight heritage. The solar panels are sized based on solar cell area and available 1U panels. Solar cell string configuration is determined to meet power storage current and voltage limits. Preliminary calculations are made following the space mission analysis and design model in order to determine adequate power source design choice. Total output power is calculated to be 13.45W at zero incidence. Final components for cubesat bus and attitude control system must be determined in order to finalize power system design and meet power storage discharge requirements.

Nomenclature

	=	Total power required from solar array
	=	Required power during eclipse
	=	Required power during daylight
	=	Period spacecraft is in daylight
	=	Period spacecraft is in eclipse
	=	Efficiency of solar cells in eclipse
	=	Efficiency of solar cells in daylight
	=	Beginning of life power
	=	Solar cell output power
	=	Efficiency of solar cell
	=	Input power to solar cell
	=	Inherent degradation
	=	Incidence angle
	=	Life degradation
	=	Degradation of solar cell
	=	Lifetime of mission
	=	End of life power
	=	Area of solar arrays
e	=	Deviation from a circular orbit
a	=	Half the distance between closest and furthest point of approach
I	=	Tilt of orbital plane with respect to Equatorial plane
Ω	=	Angle from origin of longitude to direction of ascending node
ν	=	Angle between satellite and perigee

[1] Masters Student, Aerospace Engineering, danielthernan@gmail.com, AE 295A.

= Apparent size of the Earth from the spacecraft.
= Point of closest approach
= Point of furthest approach
= Coefficient to account for bulge of the Earth

I. Introduction

The basis for this project was influenced by Dr. Nagi Mansour, a heliophysiscist at NASA Ames. There is a need to improve upon our current methods of space weather study and monitoring of solar activity. Society as a whole is more dependent and reliant on modern technology and interconnected systems. Space weather events are a systematic risk to society as they can cause big disturbances in transport, power and aviation sectors [6]. The sun is frequented with eruptions and extreme activities. Coronal mass ejections are of particular interest as they are the biggest scale solar phenomenon to occur. It has been observed that earth directed Coronal Mass ejections correlate to and are the main cause of disruptions of the geomagnetic field. CMEs can cause induced currents within long distances power transmission lines, transformers, pipelines and result in damaged electrical networks, transformer meltdowns and overall economic loss [8].

Cubesats and small satellites alike have continued to become more attractive as a method for scientific study in space. Their small size and improving functionality opens up more opportunities for cost effective mission design. It is proposed that a constellation of cubesats would provide as an invaluable source of space weather study. They can provide a method of in-situ solar wind measurements at distances within 1AU as well as improve upon current CME and overall solar modeling [9].

While at this point in time, a full design, build and launch of a constellation of satellites is years away and out of scope for our project, we will focus on launching a cubesat within LEO with the capability of continuously monitoring the sun with high precision (less than a tenth of a degree of error). The scientific analysis is the responsibility of the customer. This mission will not require propulsion and the final structure will ultimately depend upon the scientific instrumentation. This review will focus on system design of cubesats and small satellite missions designed for space weather study or high precision pointing.

A. Cubesat Subsystems

1. General

A 1U cubesat with a 10x10x10 cm cube weighs 1 kg at most and is a large picot-sat by definition and a 3U cubesat (30x10x10 cm) is a Nano-sat by definition. Historically, 20% of all satellites launched are small satellites [18]. Small satellites are simpler than large satellites, but have limited capability. Basic objectives of small satellites missions are typically simple and less complex. However, as technology has developed, the capabilities of small satellites have increased, while still maintaining a low cost. Typical funding for small satellites require their design and build to be accomplished within 1-3 years [18].

2. Power

The power subsystem is responsible for providing, storing, distributing and controlling spacecraft's electrical power. Photovoltaic arrays are commonly found on spacecraft, mounted on its external structure for energy generation.

The main design drivers of the electrical power system of a spacecraft include power consumption, power distribution, eclipse duration and payload duty cycle. Table 1 displays the system drivers, what they're driven by and their impacts. Power consumption will be driven by payload requirements and will affect the solar array sizing and battery choices. Power distribution will be driven by spacecraft design and will affect the electronic power board design. Eclipse duration will be driven by the spacecraft's orbit and will affect the battery choice.

Table 1. Power system design drivers and impacts

Major Design Drivers	Driven By	Impact
Power Consumption	Payload Requirements	Solar array, battery
Power Distribution	Spacecraft Design	Power electronics, wiring
Eclipse Duration	Orbit	Battery
Bus Voltage	Spacecraft Design	Power electronics, wiring
Payload Duty Cycle	Operations Concept	Solar array, battery

3. Controls

The attitude control system of a spacecraft is responsible for orienting the spacecraft with respect to an inertial reference frame by adjusting the pitch, roll and yaw of the spacecraft. Attitude determination and command is essential, as solar panels need to be directed towards sunlight, antennas oriented towards Earth for communications, and proper orientation of scientific instruments. Attitude measurement is achieved through use of sensors and gyroscopes. Attitude correction is achieved through use of thrusters, actuators and torques. Control is implemented through embedded software.

Before choosing an adequate attitude control and demand system, system requirements such as payload requirements, pointing accuracy, maneuvering rates and frequencies, control system type, disturbance torques, size of hardware, attitude determination method, and control law must first be defined. Usage of an active or passive control method must also be determined. Passive attitude control systems, while the most economical, cannot achieve a high enough accuracy for our mission. Passive systems usually involve a hysteresis material and magnet being mounted on the cubesats, which orient the cubesats with earth's magnetic field.

The most common control systems are spin stabilized systems, 3 axis stabilized, momentum bias, and gravity gradient. For the purpose of our mission, high pointing accuracy is required for adequate imaging of the sun. We need accuracy within a tenth of a degree [5]. Out of the most common systems, 3 axis stabilized systems are the most accurate. Typical hardware are precision gyroscopes, horizon sensors, sun sensors and star trackers. The advantages of 3 axis stabilized systems include having high accuracy, no payload limitations, can adapt to mission changes and is applicable for large power requirements [3]. However, this system is usually the most expensive and requires the heaviest weight.

4. Thermal Control

The purpose of the thermal control subsystem is to ensure that all the spacecraft components remain in their designed operational temperature limits throughout the duration of the mission. It normally accounts for two to five percent of the spacecraft's weight and cost [3]. In orbit, the spacecraft is exposed to heat from the sun, the earth and heat dissipation from its electrical components. The power system is more coupled with thermal control than any other system as a result of dissipating electrical energy [3]. Spacecraft structures commonly have large temperature limits, however those limits ultimately depend on the spacecraft's instruments. For our mission, which requires a high-resolution camera and is dependent upon a control system with less than a tenth of a degree of accuracy, the thermal control system will require a lot of attention to avoid error from thermal expansion of the optics.

5. Communications

The communications system provides interaction between the ground station and the spacecraft where the mission payload data and spacecraft status are transmitted. The communication system design is dependent on the mission requirements. Common cubesat communication systems are either RF or optical based. The systems differ in order of magnitude of the signal wavelengths and size of the required antennas. While RF based systems cover larger ranges, optical systems have no restrictions of frequency and bandwidths are not vulnerable to jamming. Deciding on the type of communication system will be decided on trade studies dependent on the link range between the ground station and spacecraft orbital position and data rate [13].

II. Literature Review

A. Relevant Missions and Technology

A critical aspect of our design is the attitude demand and control system. As of now, the best means to achieve our required pointing accuracy is through use of a sun senor and gyroscope. For small spacecraft, there are coarse sun sensors and fine or medium precision sensors. Fine sun sensors assess analog current from solar cells in order to identify the direction of the sun. Coarse sun sensors incorporate a photo diode and solar cell. The SS-411 digital is the most advanced sun sensor for small spacecraft on the market, which can be seen in Table 1 along with the Micro Digital Sun Sensor. The most precise gyroscopes are mechanical and ring laser gyroscopes. After that is fiber optical gyroscopes and micro electric and mechanical systems gyroscopes are the least precise. Fiber optical gyroscopes are more commonly used in small spacecraft. A list of the most commonly used gyroscopes can be seen in Table 2. Tables 3 and 4 display different state of the art solar cells and materials that are commonly used for solar cells.

Table 2. State of the art small spacecraft sun sensors and high precision gyroscopes [11]

Tech. Name	Description	Developer	TRL Status
Sun Sensors			
SS-411 Digital Sun Sensor	World's best seller micro DSS (Accuracy= .1 degrees)	Sinclair Interplanetary (Canada)	9
Micro-DSS	2-D APS (Active Pixel Sensor) Detector Array DSS (Accuracy =.1 degrees)	TNO (Netherlands)	7
Gyroscopes			
Micro-FORCE-1	Single axis fiber optical gyro for mini satellites (BI=1deg/h)	Northrop Grumman LITEF GmbH (USA/Germany)	9
VSGA	3-axis MEMS gyro using CRS09 for micro satellites (BI =3deg/h)	AES (Japan)	7
ADIS16405BLM	Triazial inertial sensor with magnetometer for nano and pico satellites (BI=25.2deg/h)	Analog Devices (USA)	8

Table 3. State of the art cubesat solar cells [11].

Tech Type	Description	Developer	Efficiency	TRL Status
Solar Cell	Improved Triple Junction TASC	SpectroLab (USA)	27%	9 (On Orbit)
Solar Cell	Next Triple Junction (XTJ)	SpectroLab (USA)	29.50%	9 (On Orbit)
Solar Cell	BTJ/ZTJ Space Solar Cell	Emcore (USA)	27 – 29%	9 (On Orbit)
Solar Cell	Triple Junction Solar Cell 2G28 / 3G30	AzurSpace Solar (Germany)	28 – 30%	9 (On Orbit)

Table 4. Solar cell materials [18].

Cell	Silicon (Si)	Gallium Arsenide (GaAS)	Triple Junction GaAS
Theoretical efficiency	29%	23.50%	40+%
Achieved efficiency (Best Lab)	25%	21.80%	33.80%

B. Relevant Missions

After an extensive search through online databases, there are a handful of missions with similar objectives and requirements to ours, and of those, even fewer have hardware specifications published online. The MinXSS is a 3U Cubesat designed to measure the energy distribution in solar flare activity by the University of Colorado at Boulder [2]. The MinXss uses XACT, from Blue Canyon Technologies, which is 3 axis, high precision control system. The system integrates a star tracker with momentum torque rods and a reaction wheel to achieve accuracy with .007 degrees [2]. While our mission does need high precision, it does not need a star tracker. This technology is too costly and unnecessary for locating the sun. Our mission requires more precision than coarse sensors offer, yet not as much precision as the top sensors provide. Developing or finding a sun sensor half the cost and half the precision is ideal for our mission. Specifications for the MinXSS mission can be seen in the following table.

Table 5. MinXSS specifications [2].

Orbital Parameter	Requirement	Reference Orbit
Altitude	<700 km (Cubesat)	450 km x 600 km
Inclination	>35 degrees	50 degrees
Period	N/A	95.1 minutes
Eclipse	N/A	34.9 minutes
Spacecraft Size	3U	3U
Orbit Average Power	>10W	12.5

Passerone et al. discusses design solutions for a nano-satellite developed at the Politecnico di Torino. This paper discussed the cost and reliability constraints using commercial off the shelf technology for a small satellite. The satellite contained 5 solar panels, 6 battery packs, 3 cameras with different focal lengths, 5 processors on full redundancy, and 2 communication modules with different antennas.

The spacecraft must generate its own power throughout the duration of the mission. In Sunlight, at 3 sides of the satellite will be exposed to sunlight and generating power. When in eclipse, the satellite will completely rely on stored power from the batteries. To meet power constraints, they implemented a low power consumption design. Initially, the goal was to use low power commercial technology. When the desired technology was not available, they designed a system to keep systems in idle state or completely turned off when not in use.

Table 6. Power budget for Politecnico di Torino satellite [15].

Device	Duty Cycle	Peak Power	Avg. Power
PowerMgmt.	100%	20mW	20mW
Proc A&B	6%	200mW	12mW
Payload	0.50%	3.84W	21m!
TxRx	2.60%	17.2W	443mW
Total			496mW

The main power sources were triple junction GaAs solar panels, with each having MPPT based on a switching converter, which are not vulnerable to latch-up events. Six battery packs were used to drive the two independent buses. The power switches regulated voltage, selected the proper batteries, scheduled power ups and tracked latch-up events. ProcA uses a Microchip PIC. Chain B uses a TI MSP430.

A power budget can be seen in the table 6, which displays the peak power percentage, average power, and duty cycle of on-board systems. The solar panels chosen provide around .8 W to give a margin of around .3 W based on the average power, which is around .5 W.

Viscio et al. discusses a proposed mission design for the purpose of in-situ solar observation and space weather measurements at the L1 Lagrange point. The design was based on creating a low cost bus for the cubesat, which will efficiently achieve its mission. The cubesat has a 6U design, where 2U is devoted for solar sails, 2U for scientific instrumentation, and 2U for the other subsystems such as telecommunications, power, attitude determination and control, etc. The scientific instruments include a magnetometer and plasma spectrometer for plasma environment measurements, ion and neutral mass spectrometer for sampling low mass and ionized particles in the spacecraft Ram direction [13], radiation micro dosimeters to investigate space environment, and a NanoCam C1U to image the Sun. A link budget of the scientific instruments and payload was made and can be seen in table 7.

Table 7. Cubesat system budget [13].

S/S	Mass [g]	Power [W]
Structure	1500	0
EPS	500	1
TCS	300	0
CDHS	150	0.5
AODCS	500	3
Comms	250	3
P/L	1000	3
Solar sail	860	0
Total	5060	10.5

Our mission however requires no propulsion and no use of solar sails. While, it was useful to observe the process at which they conducted their trade study, they did not provide specifics on power system design. At this time, we cannot truly create such a trade study since the final payload and scientific instrument is not yet known.

III. Orbital Mechanics

A. Background

1. Classical orbital elements

In order to properly describe or design the orbit of a spacecraft, it is required to use the classical orbital elements described in the table below.

Table 7. Classical orbital elements [16].

Element	Symbol	Description
Eccentricity		Deviation from a circular orbit
Semi-major axis		Half the distance between closest and furthest point of approach
Inclination		Tilt of orbital plane with respect to equatorial plane
Right ascension of ascending node		Angle from origin of longitude to direction of ascending node
Argument of perigee		Angle between ascending node and position vector
True anomaly		Angle between satellite and perigee

2. Orbital Period

The period of the orbit can be defined by the equation:

$$= 2 \sqrt{\frac{}{}} \quad (1)$$

Where is the standard gravitational parameter between the Sun and Earth and equal to about 3.986 ∗ 10 [16].

3. Earth centered inertial frame

The Earth centered inertial frame (ECI) is the non-rotating of reference XYZ, the center of the earth as its center where the Z-axis of the ECI points toward the geographical North Pole [16].

$$\begin{bmatrix} \end{bmatrix} \cdot \begin{bmatrix} (+) ( ) & -(+) ( ) \\ (+) ( ) & + ( ) ( ) \\ (+) & \end{bmatrix} \quad (2)$$

Where,

$$= \quad (3)$$

4. Angular radius

The angular radius of the earth describes the apparent size of the earth from the spacecraft and is seen in equation 4:

$$= \left(\sin^{-1} \frac{}{} \right) \quad (4)$$

The angular radius is dependent upon the altitude of the spacecraft. As can bee seen in figure 2, the radius is indirectly proportional to the altitude.

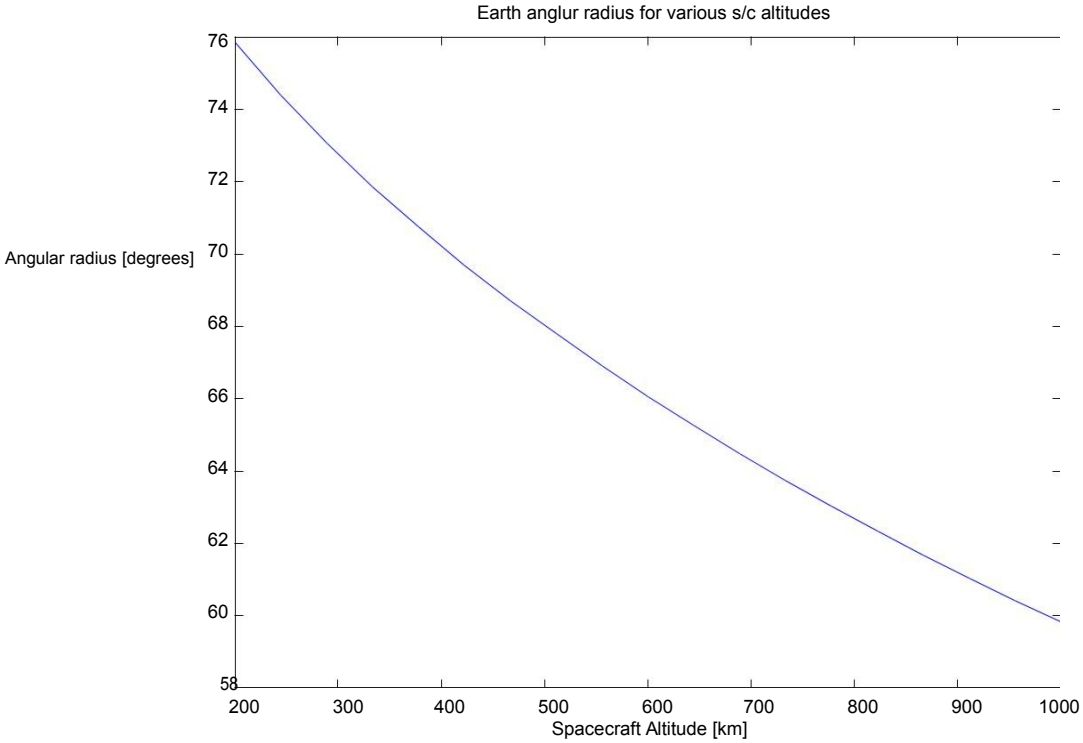

Figure 1. Angular radius of earth vs. altitude.

5. Eclipse

The time of eclipse is dependent upon the satellites period and angular radius. The relation between eclipse time and orbital period can be seen in the figure below.

$$= ! * !!^{!!} \qquad (5)$$

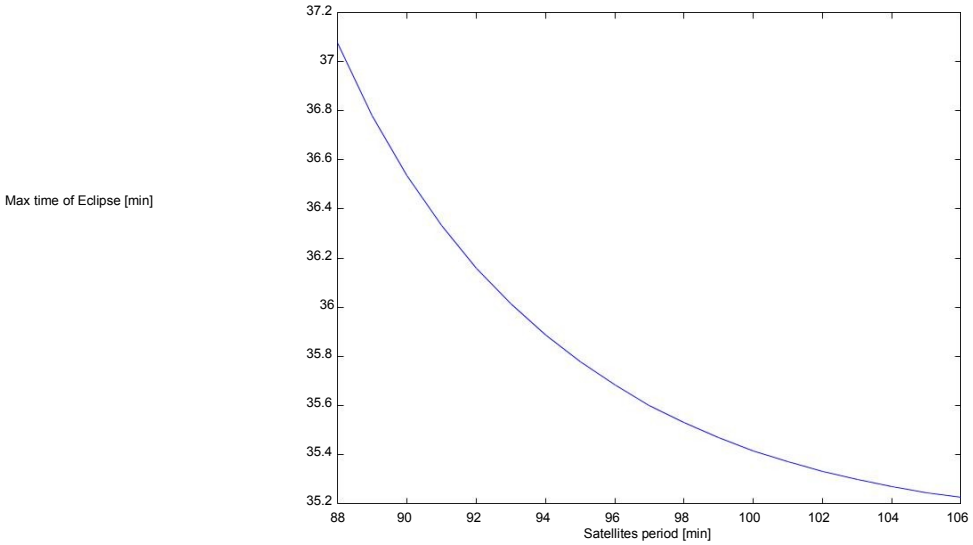

Figure 2. Max time of eclipse vs. orbital period.

6. Bulge of Earth

Earth has an equatorial bulge and is not in fact a sphere. The radius of earth is around 22km larger at the bulge (or along the equator) than at the poles. However, a spherical model is adequate enough for our calculations. The

elevation of the sun varies throughout the year. On the first day of spring, elevation is 0°. The elevation varies between $\pm 23^{\circ}$ throughout the remainder of the year. The elevation can be seen through the equation:

$$= \sin\left(\quad 2\right) \tag{6}$$

A correlation between the elevation of the sun and time of the year can be seen in figure 3. The elevation varies sinusoidally, as the azimuth is dependent on time.

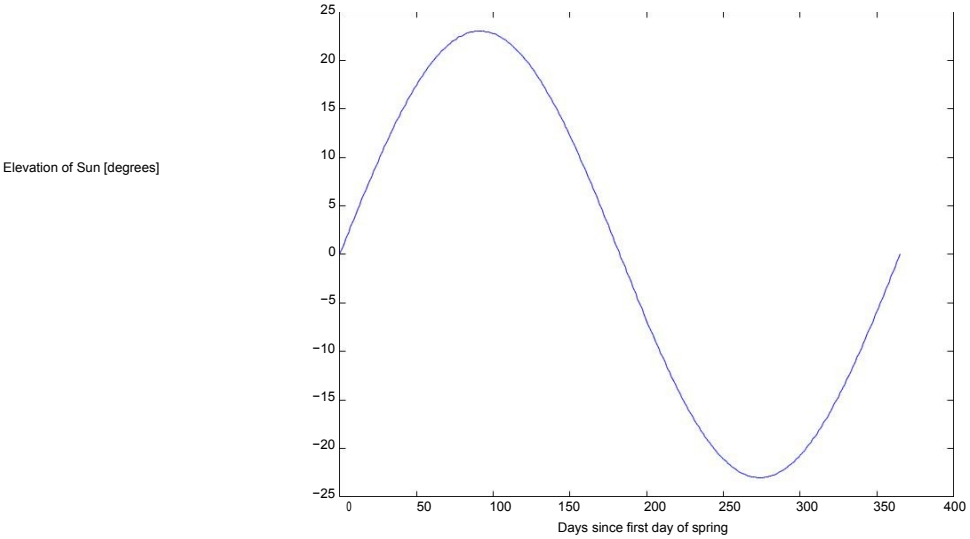

Figure 3. Sun elevation vs. days since spring.

7. Perturbations

The fundamental equation of relative two-body motion is given by:

$$= - \tag{7}$$

This is a non-linear second order differential equation, which governs motion of two point masses [16]. However, in reality a number of additional forces will affect our satellite so we will need to introduce another parameter , which is the perturbing vector.

$$= - + \tag{8}$$

Where represents perturbing forces from the Earth, Sun, Moon, atmospheric drag, oceanic tides and Earth reflected solar radiation pressure.

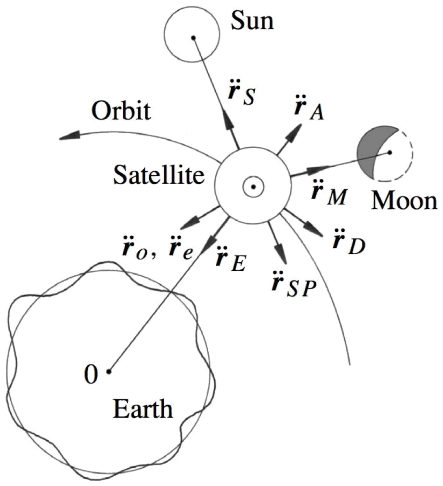

Figure 4. Perturbing forces on a satellite [17].

After atmospheric drag, the next most dominant cause of perturbation is due to the oblateness of the Earth. As the Earth is not perfectly spherical, a force of gravity on a body isn't directed towards the center of the earth (16). The dimensionless parameter, which quantifies the variation in latitude due to the oblateness of the Earth, is referred to as . For Earth

The bulge affects the right ascension of ascending node and the argument of perigee by the factors:

(9)

(10)

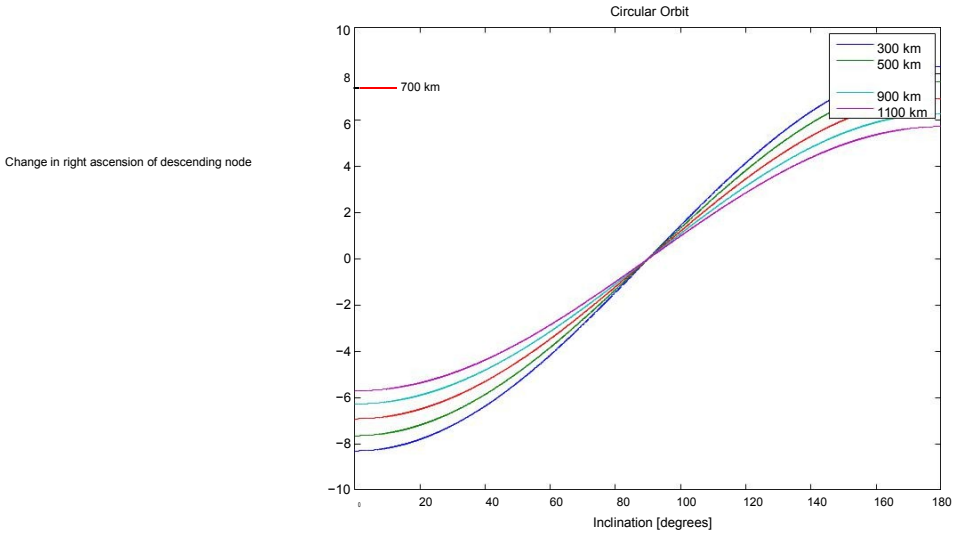

Figure 5. Change in nodal regression with respect to inclination

From the figure above, it can be seen that inclination of 90 degrees results in zero nodal regression. Inclination choices can compensate for the earth's motion around the sun and prevent the satellite from going into eclipse. It can also be seen that higher altitude orbits are less affected by the earth's bulge.

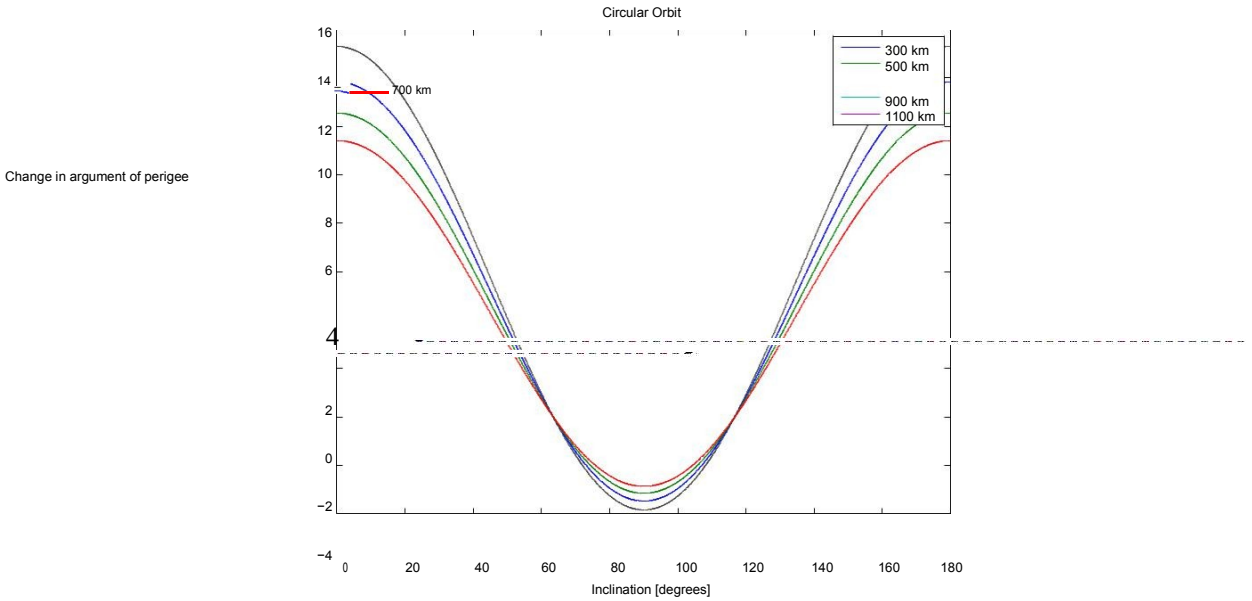

Figure 6. Change inargument of perigee with respect to inclination.

It can be seen form figure 5 and 6 that the effect of oblateness is increasing as inclination drifts from 90 degrees, where the satellite is closest to the equatorial bulge. Negative numbers for the rate of change in right ascension of ascending node correlate to westward movement and positive numbers refer to eastward movement.

8. Sun Synchronous Orbits

A sun synchronous orbit makes a constant angle with radial from the Sun to the Earth. It requires that orbital plane rotate in inertial space with angular velocity of the earth in its orbit around the sun [16]. In other words, it requires a nodal regression of:

$$= .9856°$$

At this rate, the satellites motion will compensate for eastward processing at inclinations larger than 90 degrees. . A satellite in a sun synchronous orbit has a constant view of the sun.

Noon-Midnight orbits and Dusk-Dawn orbits are special cases of Sun Synchronous orbits where the satellite flies over the same part of the earth at noon or midnight or dusk or dawn.

With proper choices of eccentricity, altitude, and inclination, a sun synchronous orbit can be achieved. Sun synchronous orbits provide optimal solar exposure for satellites, which maximizes energy production and minimizes need for energy storage.

9. Eccentricity

The eccentricity of an orbit describes the shape of the orbit and its deviation from a circular orbit. Eccentricity is zero for a circular orbit. An elliptical orbit has an eccentricity between zero and one. A parabolic orbit has an eccentricity of one and a hyperbolic orbit has an eccentricity, which is greater than one. The eccentricity can be found by dividing the difference of the perigee and apogee radius by their sum:

$$= \frac{}{} \quad (11)$$

Table 8. Eccentricity values for different type of orbits.

Orbit	Value
Circular	0
Elliptical	<1
Parabolic	1
Hyperbolic	>1

10. Semi-major axis

The semi-major axis of an orbit can be described as half the distance between the furthest and closes point of approach of an orbit [16]. The semi-major axis of an orbit can be shown through the relationship:

$$= \frac{}{} \quad (12)$$

B. Orbital Environment Calculations

1. ISS Launch

We are designing our cubesat to be launched from the International Space Station (ISS). Therefore, our cubesat will have the same orbital parameters as the ISS. This includes the apogee altitude, perigee altitude and inclination. The values of the ISS orbit can be seen in the following table. It can be seen that the perigee altitude and apogee altitude are very close leading to an almost circular orbit.

Table 9. ISS orbital values.

ISS	
Perigee	409 km
Apogee	416 km
Inclination	51.65 degrees

We can then take these values, and use equations 1, 4, 5, 8 and 9 to calculate the parameters of our cubesat's orbit. In the following table, the calculated values for semi-major axis, eccentricity, period, angular radius and time in eclipse.

Table 10. Calculated orbit values based off of ISS parameters.

Parameter	**Calculated Value**
Semi-major axis	6783.5 km
Eccentricity	0.0005
Orbital Period	5564.4 seconds (92.74 min)
Angular radius	69.92 degrees
Time in eclipse	2161.3 seconds (36 min, 38% of orbit)

IV. Power Regulation

Due to the dynamic environment in LEO, the temperature is constantly changing. For a self-sustaining spacecraft, the efficiency of the solar cells vary with temperature. There are shifts in the maximum power point of solar cells. In order to account for these variations due to temperature, a specific topology must be implemented into the electrical power system. In 2006, Clyde Space Ltd. presented a report covering the three commonly used power systems implemented on cubesats; direct energy transfer with battery bus, direct energy transfer with regulated bus, and maximum point tracker with battery bus.

Direct energy transfer with battery bus is the most simple of the three and requires the smallest mass. However, the design requires larger solar arrays resulting in a larger spacecraft mass as it lacks in operational efficiency. While this design requires less mass and volume for the actual bus, it requires more mass and volume of the overall spacecraft. A design flaw in coupling the solar array and battery restricts its optimum performance. The maximum power point of the solar array's current and voltage asynchronously increase and decrease with temperature, which results in the maximum power output occurring when the battery is completely charged [4].

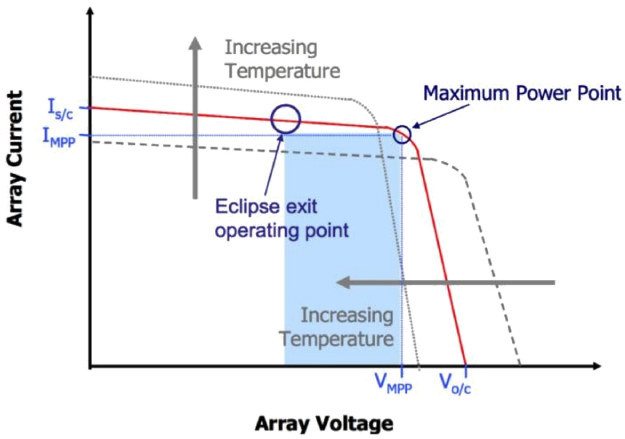

Figure 8. Rough design of 3U cubesat and opened

Direct energy transfer with regulated bus is commonly found on European spacecrafts. The design introduces a subsequent bus regulator, which regulates bus voltage during sunlight and is best suited for a spacecraft that experiences extended periods of sunlight and eclipse. This design again suffers from inefficiencies in LEO, as it doesn't operate at optimum potential unless at max temperature and at its end-of-life. However, this design has proved to be efficient in GTO or GEO [4].

The maximum power point tracker with battery steps down the solar array voltage to bus voltage using a control loop. The tracker

Figure 7. Temperature effects on solar cell I--V curve [4].

observes the max power point of the solar array and charges the battery at maximum power conditions. When fully charged, the current from the battery discharges and limits the voltage supply from the array. The power of the array is maximized in this topography, yet it suffers from a five to ten percent loss of power [4]. This design is most effective with applications that experience significant changes in maximum power point as in LEO, yet are insufficient in GEO applications.

V. Sizing and Configuration

A. TASC Solar cells

Spectrolab TASC (Triangular Advanced Solar Cells) were chosen as the solar cells to be used for power generation of our cubesat. TASC solar cells are low cost, efficient and provide four times higher voltage compared to silicon solar cells. In fact, one of the multi-junction solar cells can generate the voltage of five silicon solar cells in series. They are also twice as efficient and can produce twice the power for the same area. A big part of the selection process for the TASC solar cells involved flight heritage. TASC solar cells were flown on other university cubesats including the TechEdSat cubesats. The datasheet for the TASC solar cells can be found in Appendix A.

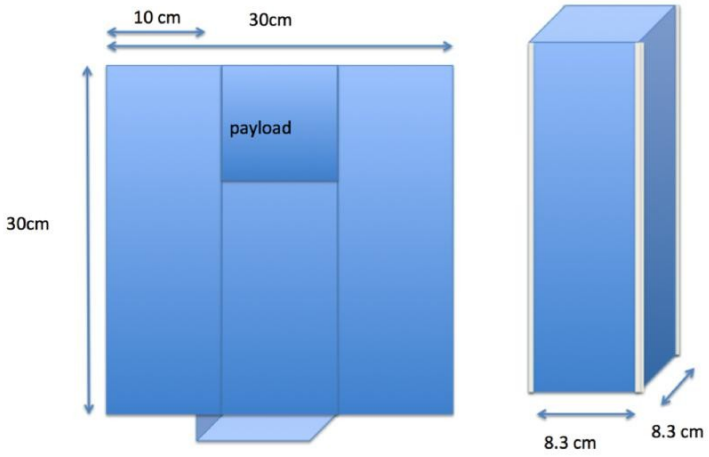

B. Solar Panel Sizing

1. Cubesat Design Specifications

The cubesat standard was defined by Cal Poly, San Luis Obispo and Stanford University to assist universities in designing and building low cost nano-satellites. These standards enforce restrictions on weight, size, and operations. There are P-Pod rails used to hold the cubesat during launch, which restrict the area on the faces of the cubesat. On four longitudinal faces of the cubesat, the area is restricted to 8.3 cm by 10 cm per 1U panel. This allows for 0.0083^{1} per 1U panel.

2. Panel Design

After selecting the TASC solar cells, the panels need to be sized. With fully deployed solar panels, there is an available area of nine 1U panels, which would be facing the sun the entire time the cubesat is in sunlight. Designating 1U for the payload of the cubesat leaves 8Us available for solar cell placement. Taking into account the area of each solar cell and design choices from universities who have used TASC solar cells, it was found that 10 pairs of solar cells (or 20 cells) could be fitted per 1U panel. This allows for 160 cells for available 8Us or 80 pairs of solar cells.

3. Cell Configuration

The next step after determining the number of cells is to determine the configuration that the cells will be connected. This will be based off the input voltage and current limits by power storage system. The BP-930 battery input voltage is 7.2V and the input current is 3.7A. The datasheet can be found in Appendix C.

Every pair of cells connected in series is considered a string. The voltage of a string cannot exceed the battery voltage. The highest potential voltage, which a single solar cell can reach, is its open circuit voltage or . The max power voltage of a TASC cells is 2.19V. The max current from a TASC cells is 31 mA. With two cells connected in series, the voltages are added to get the battery input. Based on the data sheet specifications, the input voltage will be around 5.04V using the max voltage. This is below the battery input voltage. The max current each string will produce is 31mA. For 10 strings on 8 1U panels, the total input current to the batteries will be 2480mA, which is below the battery input current requirement. Therefore, the configuration displayed in figure 9 is adequate to not exceed the power storage requirements.

Figure 9. Solar cell string configuration.

VI. Power Production

A. SMAD Model

1. Theory

Following the Space Mission analysis and Design model, we can correctly size our power generation to determine if the allotted area is adequate to supply power for the cubesat bus. We can calculate the total power required of a cubesat solar panel using the equation:

(13)

Where is the required power during eclipse and is the required power during daylight and are the periods in which the spacecraft is in daylight or eclipse. represent the efficiency of the solar array during daylight and eclipse. The values for the two depend on the method of power regulation. Efficiency in peak power tracking is lost through converters.

Table 11. Solar cell eclipse and daylight efficiency [Wertz].

	DET	PPT
	0.65	0.6
	0.85	0.8

(14)

(15)

The input power for a solar cell is 1368 / [18]. This is the amount of energy received atop the earth's atmosphere for a surface, which is directed normal to the sun. The output power of a solar cell can be calculated using:

At BOL, the power per unit area of the solar can be calculated through the equation:

Where is the inherent degradation, or efficiency lost due to manufacturing. A typical value for inherent degradation is 77%. is the incidence angle between the solar intensity vector and the spacecraft surface normal vector. This angle will vary throughout the orbit and different panels can have different incidence angles.

Whether it is from radiation or from photons trapped in the earth's magnetic field, solar cells face degradation over time. For a gallium arsenide solar cell, degradation is about 2.75% per year in LEO. The life degradation of a solar cell can be shown through the equation:

(16)

Where D is the degradation of the solar cell and L is the lifetime of the mission. The end of life power of a solar cell can be found by multiplying the beginning of life power by the life degradation.

$$!"\# = !"\# * !$$ (17)

Dividing the total power required of the cubesat solar panel by the end of life power, we can obtain the total solar array area needed to supply to the cubesat with power for the duration of the mission:

$$= \frac{!"}{!"\#}$$ (18)

Since we have not yet decided on every component of the cubesat's different subsystems, we cannot yet obtain an official amount of power needed from the cubesat during daylight or eclipse, nor can we properly determine if our current configuration is adequate. A model was provided to us by the authors of the SMAD textbook, which entails an intricate spreadsheet based on the above equations, amongst others, to adequately size the solar generation unit of the power system. A screenshot of the model can be seen in the Appendix D.

2. Preliminary Calculations

In order to make preliminary calculations, assumptions had to be made for cell efficiency, inherent degradation, degradation and incidence angles. Two different values of incidence angle were used. The first was at zero incidence and the second was to see the effects using a worst-case scenario of twenty three degrees. The assumption values can be seen in Table 12. The values for efficiency were taken from the data sheet of the TASC solar cells in Appendix A. The input power was taken from the Space Mission Analysis and Design handbook. Inherent degradation and degradation were both taken from the SMAD handbook as well.

Table 12. Assumptions for Preliminary sizing calculations

Assumptions	Worst Case	Zero incidence
Cell efficiency	27%	27%
Input power [w/m^2]	1368	1368
Inherent degradation	0.77	0.77
Degradation	2.75%	2.75%
Incidence angle [deg]	23	0

Table 13. Results for preliminary sizing calculations

Results	**Worst Case**	**Zero incidence**	**Difference**
Pout [w/m^2]	369.36	369.36	0
PBOL [w/m^2]	261.8	284.41	7.95%
LD	0.975	0.975	0
PEOL [w/m^2]	254.6	276.6	7.95%
Area [m^2]	N/A	N/A	

The flowing table displays the results of those calculations using the SMAD model. The power output density was calculated, beginning of life power density, life degradation and end of life power density for both incidence angles. Between both angles, there is only an eight percent difference between beginning of life and end of life power at zero and worst-case incidence angles.

However, at this point in time, the most important parameter is the required area of the solar cell and it cannot be determined. As it was pointed out in the previous section, the total output power of the solar array and required area is dependent upon the required power draw during eclipse and daylight. In order for this information to be determined, the final list of components and power budget needs to be decided upon.

B. Available Energy

The production of energy of the cubesat relies on the area of solar cells, the efficiency of the solar cells, the sun's radiation intensity and the incidence angle at which the sunlight strikes the cells.

$$= ! * *$$ (19)

Where ! is the intensity of solar radiation, is the effective area of the solar cells and is the efficiency of the solar cells.

1. Angle of incidence

The angle of incidence, , is the angle at which sunlight strikes a particular surface of the satellite. It is measured from normal incidence at zero degrees, to perpendicular incidence at 90 degrees. Area is a function of the angle of incidence.

$$= \ \ast \cos( ) \quad (20)$$

is the area of solar cells on one side of the satellite. At zero degrees of incidence, the sunlight

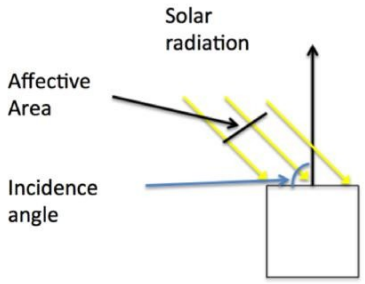

Figure 10. Solar radiation, incidence angle and effective area.

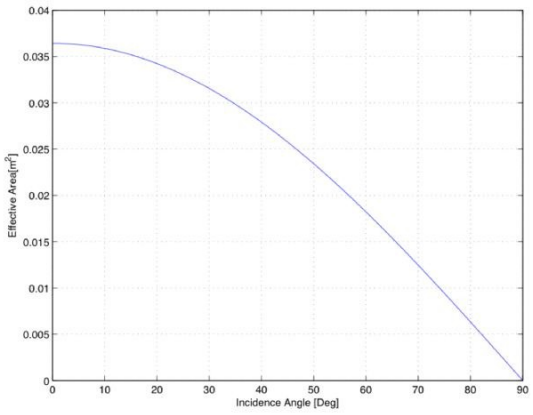

Figure 11. Effective area vs. Incidence angle.

reaches the highest potential effective area. As the angle of incidence increases away from the perpendicular, a smaller effective area is available.

Figure 12 displays the relationship between effective area of solar cells on one face of the cubesat and the incidence angle at which the sunlight strikes the surface. The effective area of the cubesat was chosen to be 0.036 . It can be seen that the effective area is indirectly proportional to the incidence angle. A higher incidence angle results in a lower amount of effective area.

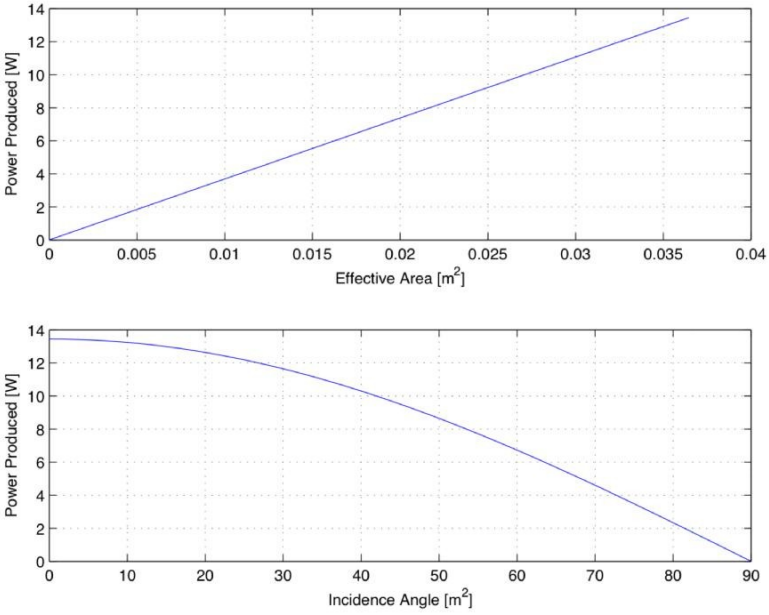

Figure 12. Power production vs. Effective area and incidence angle.

2. Preliminary Calculations

Using the efficiency of the TASC solar cells, the total available solar cell area calculated in the solar panel sizing section, and the solar radiation intensity provided by SMAD, we can see the relationship between energy produced, incidence angle and effective area. It can be seen that energy production is directly proportional to the effective area and indirectly proportional to the incidence angle.

The efficiency of the solar cell, , is a nominal value given by manufacturers in data sheets. However, this efficiency is also a function of incidence angle as well, (,). For preliminary calculations, it is adequate to assume a nominal efficiency for solar cells. However, more theory is needed in order to obtain transmission coefficients and properly account for rotation of the satellite over time. The maximum output power at zero incidence and maximum effective area was calculated to be 13.45W.

VII. Future Work

Final system components for the spacecraft bus need to be decided upon in order adequately size and design the power generation unit of the cubesat. At this point in time, the final components and design of the attitude control system has yet to be determined as well. Once these choices are made, we will determine if our current design meets the battery discharge requirements of the power storage unit as well as properly supply energy to the spacecraft bus. This will be accomplished by using the SMAD model. A larger selection of solar cells will also be investigated. Once the power generation unit is properly sized, the printed circuit board will need to be designed. This will be achieved through use of free, open source CAD software. The solar panels will then be tested to ensure that they meet the specifications provided by the manufacturer's datasheets as well as to observe their functionality with the rest of the spacecraft bus. The power control board will then be designed in order to properly distribute power through the spacecraft bus.

References

[1] Ali, A., Mughal, M.R., Ali, H., "Innovative power management, attitude determination and control tile for CubeSat standard NanoSatellites," *Acta Astronautica,* Vol. 96, No. 0, 2014, pp. 116-127.

[2] "BCT." BCT. Blue Canyon Technology, 2013. Web. 26 Feb. 2015. <http://bluecanyontech.com/all_products/cubesats/>.

[3] Brown, C.D., and ebrary, I., "Elements of spacecraft design," *AIAA education series,* American Institute of Aeronautics and Astronautics, Inc., Reston, Va., 2002, pp. 606.

[4] Clark, C., and Mazarias, L., "Power System Challenges For Small Satellite Missions," Clyde Space Ltd., 6.01 Kelvon Campus, Scotland, 2006.

[5] Erlank, A., Steyn., "Arcminute Attitude Estimation for CubeSats with a Novel Nano Star Tracker," International Federation of Automatic Control, Stellenbosch University, South Africa, 2014.

[6] Hapgood, Mike. "Space Weather: Its Impact On Earth and Implications For Business." Lloyd's. RAL Space, 2010. Web. 22 Feb. 2015. <http://www.lloyds.com/~/media/lloyds/reports/360/360%20space%20weather/7311_lloyds_360_space%20weather _03.pdf>.

[7] Ian, Poole. "Radio Waves and the Ionosphere." Nature 154.3909 (1944): 413. Staines TW18 2PW, Nov. 1999. Web. 2 Feb. 2015.

[8] Kai-Rang, W., Jun, L., Lian-Guang, L., "A Statistical Study on the Geomagnetically Induced Current Events Driven by Earth-directed Full-Halo Coronal Mass Ejections," *Chinese Astronomy and Astrophysics,* Vol. 36, No. 3, 2012, pp. 261-281.

[9] Mansour, Nagi, and Jeremie Meurisse. "The Potential of CubeSats for Space Weather Applications." (2014): n. pag. Research Gate. Web. 2 Feb. 2015. <http://www.researchgate.net/profile/Meurisse_Jeremie/publication/266852705_The_potential_of_CubeSats_for_space_weather_applications/links/543d47250cf25d6b1ad74a50.pdf.>.

[10] Navarathinam, N., Lee, R., and Chesser, H., "Characterization of Lithium-Polymer batteries for CubeSat applications," *Acta Astronautica,* Vol. 68, No. 11–12, 2011, pp. 1752-1760.

[11] "Small Spacecraft Technology State of the Art." Spacecraft 47.2 (2014): 150-58. Nasa.gov. Mission Design Division Staff, July 2014. Web. Feb. 2015. <http://www.nasa.gov/sites/default/files/files/Small_Spacecraft_Technology_State_of_the_Art_2014.pdf>.

[12] United States, "Code of federal regulations," National Archives and Records Administration, Washington, D.C., 199u,

[13] Viscio, M.A., Viola, N., Corpino, S., "Interplanetary CubeSats system for space weather evaluations and technology demonstration," *Acta Astronautica,* Vol. 104, No. 2, 2014, pp. 516-525.

[14] Xie, Ning. "A Miniaturized Micro-Digital Sun Sensor by Means of Low-Power Low-Noise CMOS Imager." IEEE SENSORS JOURNAL 14.1 (2014): n. pag. IEEE Xplore. IEEE. Web. Feb. 2015. <http://ieeexplore.ieee.org/stamp/stamp.jsp?arnumber=6588567>.

[15] C. Passerone, M. Tranchero, S. Speretta, L. Reyneri, C. Sansoe, D. Del Corso, Design solutions for a university Nano-satellite, in: Proceed- ings of the Aerospace Conference, 2008 IEEE, vol. no., 1–8 March 2008, pp. 1, 13.

[16] Curtis, H., "Orbital Mechanics for Engineering Students," Aerospace Engineering, Elsevier Science, Burlington, 2009, pp. 740.

[17] Seeber, G., and ebrary, I., "Satellite geodesy," Walter de Gruyter, Berlin; New York, 2003, pp. 589.

[18] Wertz, J.R., and Larson, W.J., "Space mission analysis and design," Space technology library, Kluwer Academic, Dordrecht, Netherlands; Boston, 1991, pp. 811.

[19] CubeSat Design Specification Rev. 12,The CubeSat Program, Cal Poly SLO

Appendix A

Spectrolab

Photovoltaic Products www.spectrolab.com

Triangular Advanced Solar Cells (TASC)

Product Description & Applications

- Designed for high power terrestrial applications, where space is at a premium.
- Two solar cells can be arranged within an approximate rectangular area of 0.611 x 1.254 inches (1.55 x 3.18 cm) with a cell gap of 0.018 inches (0.46 mm). See picture.
- Each solar cell is ideally matched to charge a single 1.2 V battery cell (eg. Ni-MH, NiCad, etc.). Cells can be wired in parallel for increased current. Two solar cells in series can charge one 3.6V Li-ion battery cell.
- A major advantage using these solar cells compared to silicon cells is that they deliver greater than 4 times higher voltage. Therefore, only one of Spectrolab's multi-junction solar cells is required to generate the same voltage as 5 Si solar cells connected in series
- Compared to typical silicon cells, these solar cells are ***over twice as efficient*** and thus will deliver more than twice the power for the same area.
- Uses and applications: A variety of power-consuming electronic equipment can benefit from these cells, especially if the area available is small or the time required for charging is limited. For example, these cells help power devices used during business trips, emergency situations or for the outdoor activities.

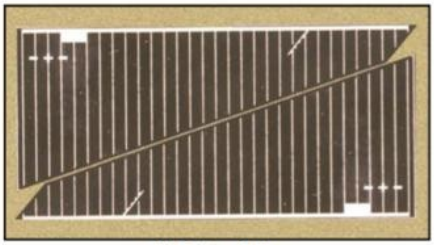

Not Actual Size

Typical Cell Electrical Parameters

1 Sun, AM1.5G (100.0 mW/cm²) 25°C

I_{sc}= 31 mA	I_{mp}= 28 mA
V_{oc}= 2.52 V	V_{mp}= 2.19 V
P_{mp}= 0.027 W/cm²	Cff= 80 %
Efficiency= 27 ± 3% Absolute	Temp. Coeff. V_{mp} = -6.2 mV/°C

Typical Cell I-V Curve (AM 1.5G)

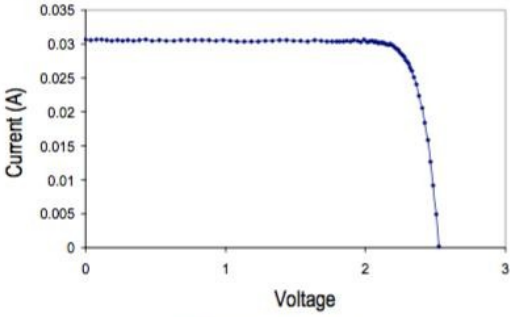

Product Description

Cell Type	Improved triple-junction gallium arsenide
Method of Cell Growth	Metal Organic Vapor Phase Epitaxy
Polarity	n/p
Thickness	190 µm (0.0075 in.)
Area	2.277 cm² (0.353 sq. in.)
Mass	0.234 g
Assembly Methods	Soldering, welding, metallized epoxy
Device Design	Monolithic, two terminal triple junction. n/p $GaInP_2$, GaAs, and Ge solar cells interconnected with two tunnel junctions.
Antireflective Coating	Multi-layer providing low reflectance over wavelength range 0.3 to 1.8µm.

ISO9001:2000 REGISTERED

SPECTROLAB

A BOEING COMPANY

The information contained on this sheet is for reference only. Actual specifications for delivered products may vary. 4/10/02

Spectrolab Inc. 12500 Gladstone Avenue, Sylmar, California 91342 USA • Phone: 818.365.4611 • Fax: 818.361.5102

Appendix B

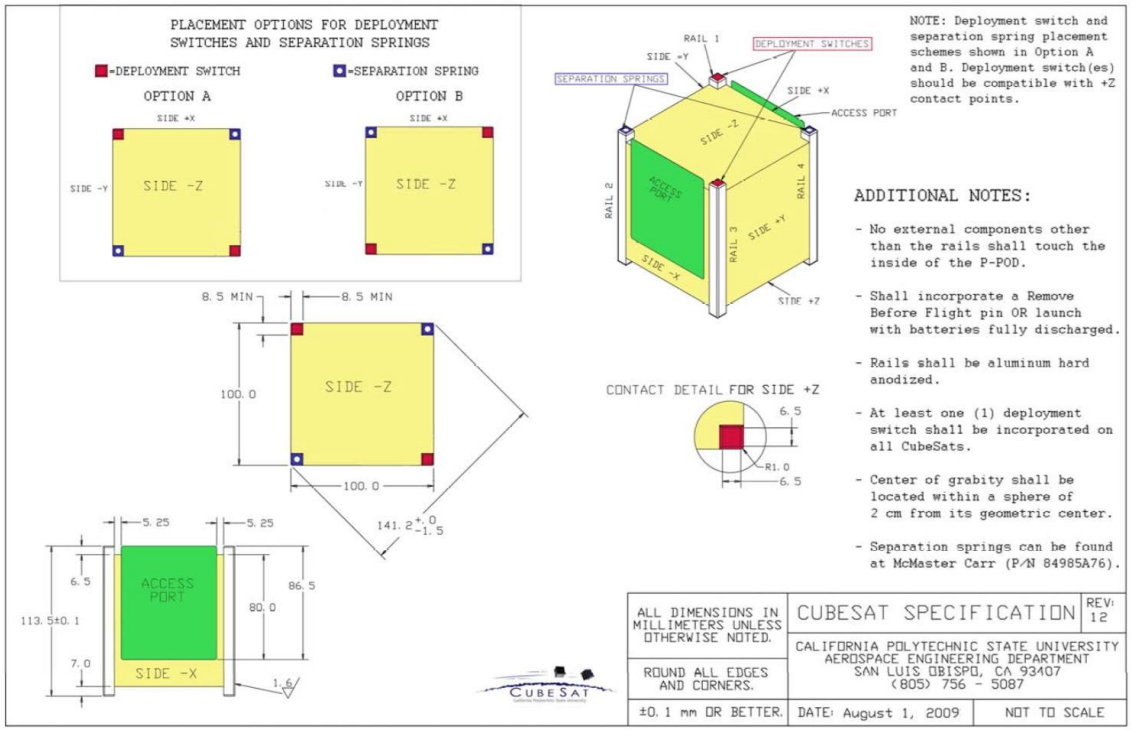
PLACEMENT OPTIONS FOR DEPLOYMENT SWITCHES AND SEPARATION SPRINGS
=DEPLOYMENT SWITCH
=SEPARATION SPRING
OPTION A
OPTION B
SIDE +X
SIDE -Y
SIDE -Z
8.5 MIN
8.5 MIN
100.0
100.0
141.2 +0 -1.5
5.25
5.25
6.5
ACCESS PORT
86.5
80.0
113.5±0.1
7.0
SIDE -X
1.6
RAIL 1
SIDE +Y
DEPLOYMENT SWITCHES
SEPARATION SPRINGS
SIDE +X
ACCESS PORT
SIDE -Z
RAIL 2
RAIL 4
RAIL 3
SIDE +Y
SIDE -X
SIDE +Z
CONTACT DETAIL FOR SIDE +Z
6.5
R1.0
6.5
NOTE: Deployment switch and separation spring placement schemes shown in Option A and B. Deployment switch(es) should be compatible with +Z contact points.
ADDITIONAL NOTES:
- No external components other than the rails shall touch the inside of the P-POD.
- Shall incorporate a Remove Before Flight pin OR launch with batteries fully discharged.
- Rails shall be aluminum hard anodized.
- At least one (1) deployment switch shall be incorporated on all CubeSats.
- Center of grabity shall be located within a sphere of 2 cm from its geometric center.
- Separation springs can be found at McMaster Carr (P/N 84985A76).
ALL DIMENSIONS IN MILLIMETERS UNLESS OTHERWISE NOTED.
ROUND ALL EDGES AND CORNERS.
±0.1 mm OR BETTER.
CUBESAT SPECIFICATION
REV: 12
CALIFORNIA POLYTECHNIC STATE UNIVERSITY
AEROSPACE ENGINEERING DEPARTMENT
SAN LUIS OBISPO, CA 93407
(805) 756 - 5087
DATE: August 1, 2009
NOT TO SCALE
CUBESAT

Appendix C

CANON BP-930 Battery
· Exceed Original Specifications !

Battery Weight : 225g

Battery Chemistry : Li-ion

Voltage : 7.2V

Battery Capacity : 3700mAh

Battery Color : Black

Product Number : VCN004

Dimensions : 70.80x38.55x39.2

High capacity, Longer Record Ti

Appendix D

	A	B	C	D	E	F	G	H	I	J
1	Return to Navigator		**Power Subsystem - Solar Array Sizing**							
2			***(All information on this sheet is contained in the block from Cell A1 to Cell I26)***							
3										
4	Required spacecraft power - sunlight	*20.0*	**20.0**	**W**		Total required solar power		**30.3**	**W**	
5	Required spacecraft power - eclipse	*5.0*	**5.0**	**W**		Controlled spacecraft power	*23.2*	**23.2**	**W**	
6						Converted spacecraft power	*23.2*	**23.2**	**W**	
7	Orbit period	*92.343*	**92.3**	**min**						
8	Maximum eclipse time	*36.0*	**36.0**	**min**		Ideal solar cell performance		**369.1**	**W/m^2**	
9	Mission duration	*1.000*	**1.000**	**yrs**		BOL power capability		**261.6**	**W/m^2**	
10						EOL power capability		**254.4**	**W/m^2**	
11	Solar flux	*1367.0*	**1367.0**	**W/m^2**						
12	Worst-case Sun incidence angle	*23.00*	**23.00**	**deg**		Required solar array area		**0.12**	**m^2**	
13										
14	Transmission efficiency - sunlight	*80.0%*	**80.0%**							
15	Transmission efficiency - eclipse	*60.0%*	**60.0%**			**Solar Array Mass & Power Budgets**				
16								Mass (kg)	Power (W)	
17	Ideal solar cell efficiency	*27.0%*	**27.0%**							
18	Inherent degradation	*77.0%*	**77.0%**			Solar Arrays				
19	Solar cell degradation per year	*2.75%*	**2.75%**			Deployed		**1.2**		
20	Lifetime degradation		**97.3%**			Cylindrical, body-mounted		**3.8**		
21						Omnidirectional, body-mounted		**4.9**		
22	Solar array power density	*25.0*	**25.0**	**W/kg**		Power Control Unit		**0.5**		
23	Spacecraft dry mass	*3.5*	**3.5**	**kg**		Regulator/Converters		**0.6**	**4.6**	
24	Percent of spacecraft dry mass for wiring	*4.0%*	**4.0%**			Wiring		**0.1**	**1.5**	
25	Percent of spacecraft power for wiring	*5.0%*	**5.0%**							
26										

	A	B	C	D	E	F	G	H
1	Return to Navigator	**Power Subsystem - Secondary Battery Sizing**						
2	***(All information on this sheet is contained in the block from Cell A1 to Cell H15)***							
3								
4	Orbit period	*92.4*	**92.4**	**min**				
5	Maximum eclipse time	*36.1*	**36.1**	**min**				
6	Mission duration	*1.000*	**1.000**	**years**				
7								
8	Required power during eclipse		**5.0**	**W**				
9	Transmission efficiency		**90.0%**					
10	Number of charge-discharge cycles		**5690**					
11	Depth of discharge		**62.4%**			Battery capacity	**5.4**	**W-hr**
12						Battery capacity	**0.2**	**A-hr**
13	Energy density		**50.0**	**W-hr/kg**				
14	Bus voltage		**28.0**	**V**		Mass of batteries	**0.1**	**kg**
15								
16								
17								